Astrophys Space Sci (2014) 353:395–404
DOI 10.1007/s10509-014-2052-2

ORIGINAL ARTICLE

Toroidal quarter waves in the Earth's magnetosphere: theoretical studies

Jayashree Bulusu · A.K. Sinha · Geeta Vichare

Received: 22 April 2014 / Accepted: 8 July 2014 / Published online: 18 July 2014

Abstract An analytic model has been developed for toroidal quarter wave (QW) oscillations in the Earth's magnetosphere using idealistic and highly asymmetric ionospheric boundary condition. The background magnetic field is dipolar and plasma density distribution is governed by a power law $1/r^m$ where r is the geocentric distance of any point along the field line and m is the density index. The solution thus obtained has been compared with the numerical solutions. Earlier workers had developed the analytic model for trivial $1/r^6$ ($m = 6$) type of plasma density distribution along the field line for which the period of the fundamental is twice that of corresponding half wave (i.e. toroidal oscillation in the symmetric ionospheric boundary). The present analytic model does reproduce this feature. In addition, it is seen that this ratio decreases for lower values of m. Moreover, for a particular value of m, this ratio shows a decreasing trend with increased harmonic number. The spatial characteristics of QW obtained from present analytic model are in excellent agreement with those computed numerically, thereby validating the model. The departure of frequency computed analytically from that obtained numerically is significant only for the fundamental and this departure reduces sharply with the increased harmonic number. It should be noted that there is no such departure for $1/r^6$ type of plasma density distribution and spatial structures as well as frequency computed from the present analytic model match perfectly with those computed numerically.

Keywords Geomagnetic pulsations · ULF waves · Field line oscillations · Quarter waves

J. Bulusu (✉) · A.K. Sinha · G. Vichare
Indian Institute of Geomagnetism, Plot No. 5, Sector-18, Kalamboli Highway, New Panvel(W), Navi Mumbai, Maharashtra, 410218, India
e-mail: bulusujayashree@gmail.com

1 Introduction

Geomagnetic pulsations, observed on the ground, are considered as the long-period (10–100 s) magnetic field fluctuations in space. The first real understanding of the geomagnetic pulsations was put forth by Dungey (1954) who proposed that the long but regular periods of these oscillations might be the result of standing Alfvén waves being excited on the geomagnetic field lines. Under the magnetohydrodynamic (MHD) approximation, these oscillations can be categorized as shear Alfvén mode and fast compressional mode (Dungey 1968). In shear Alfvén mode the perturbation magnetic field is strictly transverse to the ambient field and energy is guided along field line, whereas the fast mode has a component along the ambient field and energy moves in the direction of the wave vector, which can make any angle with the ambient field. The background nonuniform magnetic field couples the two modes (Lanzerotti and Southwood 1979). The coupling of the fast compressional mode with shear Alfvén mode within the magnetosphere has been discussed by Leonovich (2001) in an axially symmetric magnetosphere. He obtained the spatial structure of the resonant Alfvén waves within the magnetosphere and compressional wave exciting them in the solar wind region near the magnetosphere. He showed that as compressional oscillations penetrate deep into the magnetosphere, their amplitude decreases several orders of magnitude. Recently, Waters et al. (2013) reported that the Hall conductance in the ionosphere can couple shear Alfvén waves trapped in the Ionospheric Alfvén Resonator (IAR) to fast mode waves that propagate across the ambient magnetic field in an ionospheric waveguide. The coupled equation has not been solved, even in a dipole magnetic field.

However, in the extreme limit of azimuthal wave number k_ϕ the coupled mode decouples to give rise to toroidal

($k_\phi \sim 0$) and poloidal ($k_\phi \sim \infty$) oscillations characterized by azimuthal and meridional magnetic field perturbations respectively along with the compressional oscillations (Orr 1973). Leonovich and Mazur (1993) developed theory of standing Alfvén waves in the axially symmetric magnetosphere with lower azimuthal wave number and suggested that the possible source of these oscillations were the currents flowing in the ionospheric E-region. Further, they suggested that as the wave travels across the magnetic shells the poloidal mode changes to a toroidal mode. In the similar background magnetic field geometry, Klimushkin et al. (2004) suggested the criteria under which an Alfvén mode will be either toroidally or poloidally polarized. They stated that a matching of the Alfvén frequency with the eigen frequency of toroidal oscillation is necessary and sufficient for the wave to be toroidally polorized. However, for the Alfvén wave to be polarized in the poloidal direction, the wave frequency should match with the eigen frequency of poloidal oscillations and in addition, the azimuthal wave number associated with wave must be very large. They showed that the Alfvén mode was polorized in the poloidal direction for an azimuthal number of ∼50–100 when the background plasma pressure was considered small but finite.

There have been many theoretical as well as observational studies related to the toroidal and poloidal oscillations which are excited on geomagnetic field lines (Cummings et al. 1969; Anderson et al. 1990; Engebretson et al. 1986; Sinha et al. 2005; Pilipenko et al. 2005; Mager et al. 2009; Bochev and Sinha 2010; Liu et al. 2013; Takahashi et al. 2013) The conversion of poloidal to toroidal mode is reported in few studies (Mann and Wright 1995; Leonovich 2001). Mann and Wright (1995) suggested that compressional poloidal waves have finite lifetime and gradually gets converted to Alfvén waves of toroidal polarization. The time scale of this conversion depends on the azimuthal wave number associated with the wave. Similar result was discussed by Mager and Klimushkin (2006, 2007). Mager et al. (2009) developed analytic as well as numerical solution for the field aligned structure of poloidal mode oscillations under the effect of finite pressure and brought out interesting results. Thus, it is important to study and understand the field line structure of toroidal as well as poloidal modes in the Earth's magnetosphere. In this paper, we solve the problem of toroidal structures along the field line analytically in the dipole magnetic field geometry. This is not to undermine the importance of problem pertaining to poloidal oscillations, however it becomes mathematically bit more complex and will be dealt in our future communication. The numerical solution for field line structure of poloidal oscillations is trivial and straight forward. The focus of the present paper lies in the analytic model of toroidal oscillations. The analytic solution thus obtained is compared to the numerical solution to test the authenticity of the model.

The existence of the standing structure of toroidal mode depends on reasonable levels of reflection from the ionospheres at the feet of the field line. In fact, the structure and development of the waves are significantly modified by boundary conditions at the ionospheres. Depending on the ionospheric conductivity the following wave modes can be obtained: (a) Half wave and (b) Quarter wave. Half wave modes are formed when the ionospheres have symmetric conductivity at the conjugate ionospheres. These waves are likely to be observed at local noon and midnight of equinoxes (Hughes and Southwood 1976). Quarter wave (QW) modes, on the other hand, are natural standing magnetohydrodynamic (MHD) Alfvén modes excited on the geomagnetic field lines during highly asymmetric conjugate ionospheric conditions. In the present study, we discuss in detail the theoretical aspects of toroidal quarter wave oscillations in the Earth's magnetosphere.

Quarter wave modes were first introduced by Allan and Knox (1979a) who presented propagation of ULF wave resonances in dipole magnetic field for the axisymmetric toroidal oscillations. They assumed plasma distribution of $1/r^6$ type and demonstrated that at a given magnetic L-shell (characterized by McIlwain parameter L) when the Pedersen conductance is asymmetric between the two conjugate ionospheres, 'Quarter-wave' modes are formed with higher periods than the corresponding half waves. In fact, for plasma density varying as $1/r^6$, the fundamental period of quarter wave for a particular L-shell is approximately twice that of corresponding half wave oscillations.

The latitudinal profile of electric and magnetic field for different ionospheric boundary conditions were discussed in detail by Allan and Knox (1979b). They suggested that when the Pedersen conductance is asymmetric between the ends of the field line, the travelling wave component of the field line oscillations begins to dominate the standing conditions. This leads to heavily damped oscillations and an increase in the energy inflow to the ionosphere with smaller conductivity. But for strong asymmetry in the Pedersen conductivity, a quarter wave standing mode is formed with a 'near-node' of electric field in the higher conducting ionosphere and a 'near-antinode' in the lower conducting ionosphere. The condition is reversed in the magnetic field oscillation.

Behaviour of the time-integrated Poynting vector and its relation with the phase of the quarter wave was discussed in great detail for the geo-stationary orbit by Allan and Knox (1979b). It was shown that, for quarter wave, the time-integrated Poynting vector was zero at a point (termed as the 'null-point') displaced away from the equator.

Similar exercise were carried out by Southwood and Kivelson (2001) who used the WKB approximation to analyze the energy flow and the phase structure of damped Alfvén wave in a dipole field configuration. They showed that an introduction of asymmetry in the conductance leads to the shift of the null-point away from the equator. They attributed this shift to the asymmetry in the Poynting flux around the equator. They developed expressions for damping decrement for varied ionospheric conductance and showed that the frequency of oscillation depends on the length of the field line and Alfvén speed, whereas the damping decrement is a function of ionospheric conductance.

Ozeke et al. (2005) presented numerical solutions to guided toroidal and poloidal Alfvén wave equations in a dipole field geometry with asymmetric ionospheric Pedersen conductances. They showed that the direction of propagation of energy is not dependent on the distance from the ionosphere but depends on the time integrated Poynting flux. They demonstrated that the position of null point along a field line varies as a function of Pedersen conductivity and its latitudinal position on the field line is different for guided toroidal and poloidal mode.

The diurnal variations of the parameters of the magnetospheric Alfvén wave resonator at different latitudes were calculated using a semi-empirical model of ionosphere-magnetosphere plasma distributions in Cartesian geometry by Yagova et al. (1999). They established a numerical relation between the quarter wave and half wave harmonic and showed that the lowest quarter wave mode should have frequency nearly half of that of a fundamental mode for symmetric ionospheres for $1/r^6$ type of plasma distribution.

The problem of quarter wave was discussed numerically for general power law of plasma mass density distribution (Allan and Knox 1979b; Ozeke et al. 2005; Allan 1983). In their numerical approach, they considered the density variation to be governed by the power law $\rho = \rho_o(r_o/r)^m$, where ρ_o is proton mass density at r_o, the geocentric distance to equatorial crossing point of the field line considered.

There have been only a couple of observations of quarter waves till date. The first observation was reported by Allan (1983) who observed an anomalously long period pulsation event near $L = 4$ during November 1977 by using ground magnetometer data. The D component showed strongly asymmetric amplitude with 90° phase difference between conjugate points when one hemisphere was sunlit and the other was dark. Budnik et al. (1998) reported a pulsation event of 18–19 mHz, recorded by the GOES-6 satellite. It was seen that as the satellite was crossing the dusk terminator, the frequency abruptly decreased to 5–6 mHz. They assigned the frequency 18–19 mHz observed in the day side to half wave and the frequency 5–6 mHz observed around the dusk terminator to quarter wave on the basis of reflection at the ionosphere. They proposed that it is the sign of the reflection coefficient (R) at the two conjugate points that decides if a given wave is a half (similar sign of R at conjugate points) or quarter wave (opposite signs of R at the conjugate ionospheres in the two hemispheres). The reflection coefficient $R^{N,S}$ at the northern hemisphere (superscript N) and southern hemisphere (superscript S) is given by Scholer (1970) as $R^{N,S} = \frac{\Sigma_A - \Sigma_P^{N,S}}{\Sigma_A + \Sigma_P^{N,S}}$, where $\Sigma_A = \frac{1}{\mu_0 V_A}$ is the wave conductance; V_A is the Alfvén speed at the conjugate point and Σ_P is the height integrated Pedersen conductance. The latest observations of quarter waves were reported by Obana et al. (2008). They used the cross-phase analysis on ground magnetometer data of European and American sectors. They discussed properties of 7 quarter wave events and presented detailed observational and numerical simulation results for one of these events which occurred during dawn of 27 June 2001. The frequency was unusually low (15 mHz) at 0700 MLT when the interhemispheric ionospheric Pedersen conductance ratio was around 30 and increased to ~27 mHz at 1100 LT when the interhemispheric conductivity ratio decreased to 3.8. They concluded that the interhemispheric Pedersen conductance ratio should be at least 10 for the generation of a quarter wave.

Analytically, the problem of quarter wave was solved only for steep plasma distributions obeying $1/r^6$ variation along the field line by earlier workers (Allan and Knox 1979a; Southwood and Kivelson 2001; Ozeke et al. 2005). However, it is evident from previous observational studies that the density variation obey different power laws in different magnetospheric regions. For example, inside the plasma trough $m = 3$ (Carpenter and Smith 1964), outside the plasmasphere $m = 4$ (Carpenter and Smith 1964), inside the plasmasphere $m = 3.38$ (Newbury et al. 1989), $m = 0$ at low latitudes close to equatorial plane (Gallagher et al. 2000), and at the equatorial plane $m = 1$ (Goldstein et al. 2001).

Hence, there is a need to develop a convincing analytic model that can describe these oscillations in different magnetospheric regions (characterized by different L-values) for appropriate plasma distributions (characterized by suitable m-value). The correct analytic description will provide a better insight and will be important in understanding the generation mechanism of these waves. The analytic expression of normal modes can be used to study their coupling with different driving sources and all those phenomena where the field line structures are important. Sinha and Rajaram (2003) demonstrated this aspect by using Green's function technique for computing response of normal modes of half wave to sudden change with solar wind dynamic pressure.

In this paper, we have developed an analytic model of quarter wave toroidal oscillations and computed their normal modes. In Sect. 2, we present a Direct analytic model (DAM) of quarter wave developed by us, using a generalized plasma mass density distribution and idealistic ionospheric boundary conditions in dipole magnetic field. The spatial and temporal characteristics of quarter wave obtained from DAM and Numerical Exact Solution (NES) are discussed in Sect. 3. Section 4 presents the discussion and concludes our findings.

2 Theoretical background

We adopt the following second order wave equation developed by Singer et al. (1981) that describes the low frequency transverse waves in an infinitely conducting, stationary magnetized plasma with negligible plasma pressure

$$\mu_o \rho \frac{\partial^2}{\partial t^2}\left(\frac{\xi_\alpha}{h_\alpha}\right) - \frac{1}{h_\alpha^2}\overrightarrow{B_o}.\overrightarrow{\nabla}\left[h_\alpha^2 \overrightarrow{B_o}\cdot\overrightarrow{\nabla}\left(\frac{\xi_\alpha}{h_\alpha}\right)\right] = 0 \quad (1)$$

where μ_o is the magnetic permeability in vacuum, ρ is plasma mass density, ξ_α is the plasma displacement perpendicular to the field line, $\overrightarrow{B_o}$ is the ambient magnetic field. The parameter α determines the mode of oscillation and signifies the direction of plasma displacement. h_α is the scale factor for the normal separation between the field lines in the direction of α and is determined by the magnetic field geometry.

For perfectly reflecting and symmetric ionospheric boundaries, analytic as well as numerical solutions to Eq. (1) for toroidal oscillations were developed by Sinha and Rajaram (1997) in the dipole field geometry. They assumed the plasma density to vary as $1/r^m$, where m had integer values between 0–6. In the present study, we employ the same methodology to examine the eigen characteristics of quarter wave toroidal oscillations by making the necessary changes in the ionospheric boundary conditions.

The mode equation (1) is solved with the following assumptions. (a) The background magnetic field is dipolar. (b) Perturbed quantities vary as $\exp(i\omega t)$. (c) Density variation is governed by the power law $\rho = \rho_o(r_o/r)^m$, where m is the density index and ρ_o is proton mass density at r_o. r_o is the geocentric distance to equatorial crossing point of the field line considered, and r is the geocentric distance to the position of interest on the field line.

In the light of above mentioned assumptions Eq. (1) can be written in the normalized dimensionless form as

$$\frac{\Omega^2}{\sin^{2m}\theta}X + \frac{B}{h_\alpha^2}\frac{d}{dS}\left[h_\alpha^2 B \frac{dX}{dS}\right] = 0 \quad (2)$$

where $S = \frac{s}{R_E}$, $\Omega = \frac{\omega R_E}{V_{Aeq}}$, $X = \frac{\xi_\alpha}{R_E h_\alpha}$, $B = \frac{B_o}{B_{eq}}$, s is the distance measured along the field line from the equator, R_E is the Earth's radius, V_{Aeq} is the Alfvén speed at the equator, B_{eq} is the ambient magnetic field at the equator, and θ is the colatitude.

In dipole magnetic field, the parameters h_α, B, B_{eq}, are given by the following expressions. $h_\alpha = L\sin^3\theta$ for the toroidal mode, $B = \sqrt{1+3\cos^2\theta}/\sin^6\theta$, and $B_{eq} = 0.311/L^3$ Gauss. $L = 1/\sin^2\theta_c$ is the geocentric distance of the point in R_E where the field line crosses the equator. The suffix c indicates the value at the conjugate point. By solving Eq. (2) for X, an estimate of plasma displacement can be obtained and the characteristics of electric and magnetic field of quarter wave can be realized.

In order to solve for X, Eq. (2) is transformed to standard WKB form (Bender and Orszag 1978)

$$\epsilon^2 \frac{d^2X}{dv^2} + \Phi(v)X = 0 \quad (3)$$

by choosing, $\frac{dv}{dS} = \frac{1}{h_\alpha^2 B}$, $\epsilon = 1/L^2$, and $\Phi(v) = \Omega^2 \times \sin^{12-2m}\theta$. An important thing to note here is that for a density index $m = 6$, this equation reduces to simple harmonic type whose solutions are straight forward and identical to those obtained by Allan and Knox (1979a) and Southwood and Kivelson (2001).

It has been demonstrated by Sinha and Rajaram (1997) in case of half wave that the solution of the above standard WKB equation does not provide the correct analytic picture, especially in case of fundamental for which the scale length is comparable with the size of the system. They showed that the singularity in $\Phi(v)$ at turning points ($\theta \sim 0$ or $\theta \sim \pi$) is responsible for ambiguous solution near the conjugate points. In order to tackle this singularity we use Langer (1949) approach and obtained the analytic solution for X as a linear combination of standard Bessel's functions as

$$X = \sqrt{\frac{1}{2L\nu}}\sqrt{\frac{V_{Aeq}}{\omega L R_E}}\frac{\eta^{1/2}}{\sin^{3-m/2}\theta}\left[J_\nu(\eta) + K J_{-\nu}(\eta)\right] \quad (4)$$

where $\eta = \frac{\omega L R_E}{V_{Aeq}}\int_0^\theta \sin^{7-m}\theta$ and $\nu = 1/(8-m)$. $J_\nu(\eta)$ and $J_{-\nu}(\eta)$ are Bessel functions of first kind in the variable η and of order ν and $-\nu$ respectively. The solution X is a function of colatitude (θ) and provides the normalized displacement ($X = \frac{\xi_\alpha}{R_E h_\alpha}$) all along the field line. The arbitrary constant K in Eq. (4) is determined by the appropriate boundary condition at the conjugate ionospheres where the field line terminates using idealized conditions (i.e. the Pedersen conductivity is infinitely large or infinitesimally small). Symmetric boundary condition (i.e. identical conductivity at both the conjugate ionosphere) will give rise to half wave oscillations whereas asymmetric boundary condition (i.e. infinitely large conductivity at one conjugate ionosphere and infinitesimally small conductivity at the other conjugate ionosphere) will give rise to quarter wave oscillations.

2.1 Boundary conditions for quarter waves

In order to obtain the solution for toroidal quarter wave, Eq. (4) is solved under idealistic and asymmetric ionospheric boundary conditions i.e. $\Sigma_P^N \to 0$ and $\Sigma_P^S \to \infty$ or vice-versa. It should be noted that at the ionospheric boundary, electric field or magnetic field is vanishing depending upon $\Sigma_P^S \to \infty$ or $\Sigma_P^S \to 0$ respectively. Using these ionospheric boundary conditions the eigen frequency and the field aligned structure of electric and magnetic field oscillations associated with quarter wave are obtained.

The arbitrary constant K is estimated by making the solution X zero if the Pedersen conductance Σ_P is infinitely large or its derivative dX/dS zero if Σ_P is infinitesimally small at one of the conjugate points. The eigen frequency of quarter wave is obtained by reversing this condition at the other conjugate point.

It is important to note that the solution X in Eq. (4) was initially developed under the assumption that the ionosphere in both the hemispheres is infinitely conducting, resulting in the formation of half wave (Sinha and Rajaram 1997). Unlike the quarter wave, half wave is symmetric around the equator. Thus, the field line structures of electric and magnetic field oscillations associated with half wave were obtained by imposing one boundary condition at one conjugate point and the other at the equator (solution was obtained in the domain ($[\theta_c, \frac{\pi}{2}]$). The solution was replicated to the other conjugate point from the equator thus giving the complete field line structure between the conjugate points in the two hemispheres i.e. in the domain interval $[\theta_c, \pi - \theta_c]$. However, in case of quarter wave, the mode is not symmetric around the equator and the point of symmetry is shifted to the other conjugate point at $\pi - \theta_c$. Thus, the constant K in Eq. (4) is estimated at one conjugate point (say, θ_c) by making the derivative of the solution (dX/dS) or the solution (X) to vanish depending on whether the ionospheric conductivity is infinitesimally small or infinitely large. The frequency is then evaluated by applying the reverse boundary condition at the other conjugate point (i.e. at $\pi - \theta_c$).

Using the estimated constant and frequency, the normalized plasma displacement X is computed using Eq. (4). The corresponding electric and magnetic field associated with quarter wave can be obtained by using the following expression. $E_\beta = \omega \xi_\alpha B_o$ and $b_\alpha = h_\alpha B_o \frac{d}{ds}(\frac{\xi_\alpha}{h_\alpha})$ respectively, where $(\overrightarrow{B_0}/B, \hat{\alpha}, \hat{\beta})$ form a right-handed orthogonal system.

2.2 Numerical exact solution

The correctness of the solutions obtained from DAM is established by performing numerical exact solution of Eq. (2). Equation (2) can be decoupled to two first order equations as

$$\frac{dX}{dS} = \frac{1}{h_\alpha^2 B} Y \tag{5}$$

$$\frac{dY}{dS} = -\frac{\Omega^2 h_\alpha^2}{B \sin^{2m} \theta} \tag{6}$$

The two coupled Eqs. (5) and (6) could be solved numerically using second-order Runge-Kutta method. We start by considering that the derivative $dX/dS = 0$ for $\Sigma_P^N \to 0$ and the function $X = 0$ for $\Sigma_P^S \to \infty$. With these initial condition, we solved the two simultaneous equation along the field line till the other conjugate point is reached where $\Sigma_P^N \to \infty$ and $\Sigma_P^S \to 0$. Once the frequency is determined, the solution and its derivative could be obtained by solving the coupled equation. Thus, the numerical estimates of electric and magnetic field fluctuations were obtained for different modes of quarter wave toroidal oscillations. Characteristics of electric and magnetic field associated with toroidal quarter wave oscillations as obtained from the DAM and NES, are discussed in the following section.

3 Model results

3.1 Classification of harmonics for half and quarter waves

The nomenclature assigned for harmonics of half waves (formed due to symmetric ionospheric boundary condition) and quarter waves (formed due to highly asymmetric ionospheric boundary conditions) are different. The half wave consists of both odd as well as even harmonics. If n denotes the harmonic number, then the half wave mode corresponds to fundamental when $n = 1$, to second harmonic when $n = 2$ and so on.

On the other hand, the quarter waves are characterized only for odd harmonics because of the asymmetry of ionospheric conductivity. Hence, the quarter wave mode corresponds to fundamental when $n = 1$, to second harmonic when $n = 3$ and so on. It should be noted that frequencies for $n = 2$ in the quarter wave solution is identical to that for fundamental half wave, $n = 4$ is identical to second harmonic of half wave and so on. But the spatial structures are completely different for quarter and half waves. That is why for the frequencies of quarter wave harmonic, we talk of odd values of n and frequencies of successive harmonics are determined by $n = 1, 3, 5$ and so on.

3.2 Temporal behaviour of toroidal quarter waves

The quarter and half wave angular frequencies can be computed for a range of density indices from $m = 0$–6 and for different equatorial ion number densities using DAM and NES. In our analysis, we assume that protons are the only ion species as prescribed by earlier workers (Cummings et al. 1969; Sinha and Rajaram 1997). We present the angular frequencies obtained using NES (ω_E) and DAM (ω_D) in Table 1 for a typical equatorial plasma density of 1/cc, density indices $m = 5$ and $m = 6$ at $L = 6.6$. It should be noted that the model can account for different m and L-values. It is clearly seen from Table 1 that the percentage departure of DAM frequency from NES frequency $[\frac{(\omega_D - \omega_E)}{\omega_E} \times 100]$ decreases with increasing harmonic number. The departure is significant (e.g. 13.6 % for $m = 5$) for the fundamental quarter wave, which reduces significantly for higher harmonics.

Table 1 Estimated frequencies obtained for quarter wave toroidal field oscillations at $L = 6.6$

Density index m	Harmonic number HN	$\omega_{1/4}$		$T_{1/4}$		% departure of ω_D from ω_E
		DAM(ω_D)	NES(ω_E)	DAM(T_D)	NES (T_E)	$\frac{(\omega_D-\omega_E)}{\omega_E} \times 100$
5	1	0.064	0.056	97.44	111.65	13.6
	3	0.18	0.17	34.90	36.29	3
	5	0.29	0.291	21.29	21.74	1.2
	7	0.41	0.407	15.32	15.53	0.5
	9	0.52	0.52	11.97	12.08	0.1
6	1	0.048	0.048	131.22	131.22	0
	3	0.14	0.14	43.74	43.74	0
	5	0.24	0.24	26.24	26.24	0
	7	0.335	0.335	18.74	18.74	0
	9	0.43	0.43	14.58	14.58	0

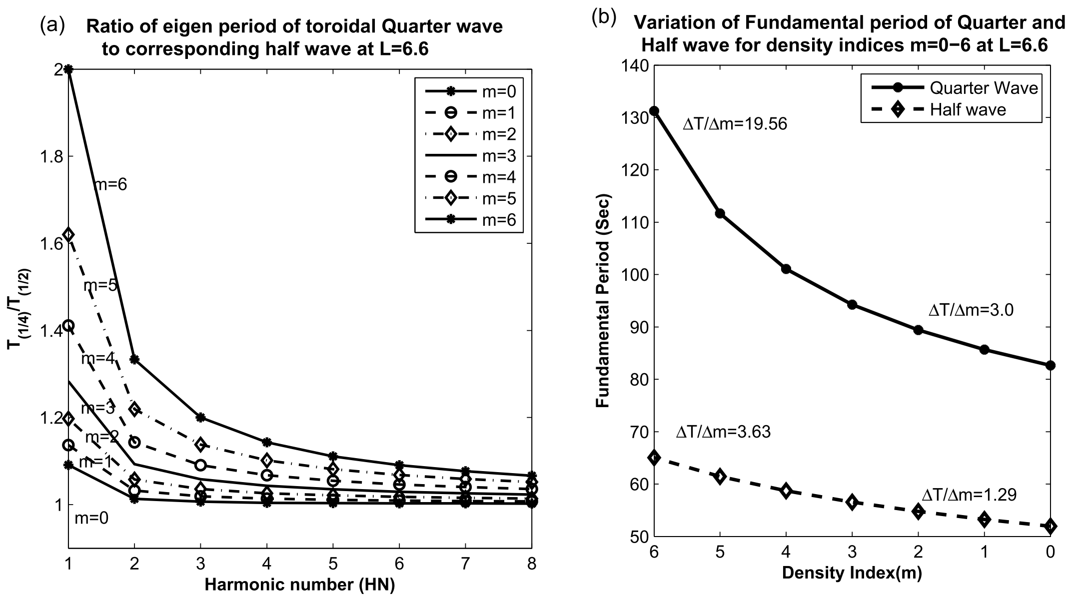

Fig. 1 (**a**) Variation of $T_{1/4}/T_{1/2}$, which is the ratio of time periods obtained from analytic solution for quarter wave to that of half wave, for density index varying from $m = 0$–6 at $L = 6.6$. $T_{1/4}$ and $T_{1/2}$ denote time period related to quarter and half wave respectively. Variable HN is the harmonic number. HN varies as $1, 3, 5 \dots$ for $T_{1/4}$ and as $1, 2, 3 \dots$ for $T_{1/2}$ respectively. (**b**) Variation of fundamental period of quarter and half wave for density indices $m = 0$–6 at $L = 6.6$ as obtained from DAM

In addition, it is clearly seen that for $m = 6$ (i.e. for $1/r^6$ type density distribution), the angular frequency obtained from DAM is identical to that obtained from NES (0% departure between ω_D and ω_E). This validates our analytic model.

The ratio of eigen period of quarter wave to that of half wave for corresponding harmonic are shown in Fig. 1a for density indices $m = 0$–6 at a typical value of $L = 6.6$. It can be seen that only for a density index of $m = 6$ and for the fundamental, this ratio is 2 as envisaged by earlier workers (Allan and Knox 1979b; Yagova et al. 1999). This can be explained as follows. The period of the toroidal mode is a function of Alfvén speed (V_A) and length of the field line. The Alfvén speed varies as $\frac{B}{\sqrt{\rho}}$, where B varies as $1/r^3$ and density ρ varies as $1/r^m$ along the field line. For a density index $m = 6$, the decrease in the magnetic field is balanced by the change in the square root of density ($\sqrt{\rho}$) along the field line. Thus, for both half wave and quarter wave, the Alfvén speed is uniform (equal to the equatorial speed V_{Aeq}) all along the field line. This can also be realized from the term $\phi(v)$ in Eq. (3). The eigen period of both quarter and half wave is controlled by the length of the field line characterized by L-value. As the fundamental quarter wave covers along the field line twice the distance as compared to half wave, the period of quarter wave to execute one cycle is

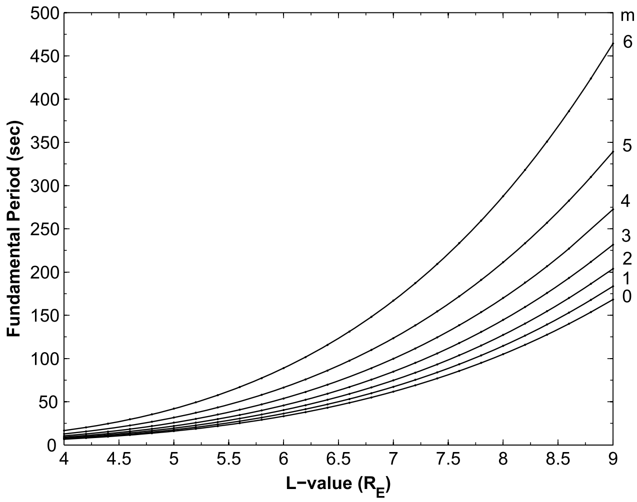

Fig. 2 Variation of fundamental quarter wave period for density index varying from $m = 0$–6 at $L = 6.6$ as computed from DAM

twice that for half wave for constant V_A (i.e. for $m = 6$) in Fig. 1a.

For density indices other than $m = 6$, the density variation ($\sqrt{\rho}$) is less steep compared to the variation of magnetic field strength along a field line. This leads to an increased Alfvén speed as we move away from equator along the field line. But the decreasing ratio of $T_{1/4}/T_{1/2}$ from Fig. 1a with density index m for the fundamental suggests that the rate of decrease of $T_{1/4}$ with respect to m is more as compared to the rate of decrease of $T_{1/2}$. This can be inferred from Fig. 1b which shows the variation of fundamental eigen period of quarter and half wave with respect to density indices $m = 0$–6 at $L = 6.6$. It can be seen that the rate of decrease of fundamental period with density index m ($\Delta T/\Delta m$) is steeper in case of quarter wave as compared to half wave. For quarter wave, $\Delta T/\Delta m$ is 19.56 between $m = 6$ to $m = 5$ which decreases to 3.0 between $m = 1$ and $m = 0$. However, for half wave this rate is 3.63 between $m = 6$ and $m = 5$ and reduces to 1.29 between $m = 1$ and $m = 0$.

Another interesting fact to be noted here is that even for density index $m = 6$, the ratio of second harmonic of quarter wave with the corresponding half wave decreases as compared to the fundamental [Fig. 1a]. The decrease is steep from fundamental to the second harmonic of quarter wave and the steepness decreases with decreased m and increased harmonic number of quarter wave characterized by n. The ratio saturates beyond certain n depending upon the density index m. The saturation level is high for higher m.

Figure 2 depicts the change in the fundamental quarter wave period as obtained analytically over a range of magnetic shells ($L = 4$–9) for density index $m = 0$–6. It is seen that the fundamental period of quarter wave increases with the density index m. As m increases, the density decreases steeply along the field line. This reduces the Alfvén speed of the wave, thereby causing an increased period of the wave. For a given density index m, the period increases with L. This is because with increasing L, the length of the field line increases resulting in the increase of the wave period.

3.3 Field aligned structure of quarter waves

The field line structures of electric and magnetic field fluctuations associated with toroidal quarter wave oscillations for the first three harmonics are shown in Figs. 3 and 4 respectively. The top three panels in Fig. 3 show the latitudinal variation of the electric field for a density index of $m = 4$ at $L = 6.6$ for the first three harmonics of quarter wave, the middle three panels show the electric field variation for a density variation of $m = 5$ and the bottom three panels represent the electric field variation for density index $m = 6$. The solid and dotted curve mark the solutions computed from analytic and numerical method respectively. The electric field variation computed analytically shows excellent agreement with the numerical solution for density indices $m = 4$ and $m = 5$. For $m = 6$, these two curves coincide exactly.

The number of nodes formed along the field line are decided by the harmonic number of the quarter wave. Another interesting fact one can decipher from Fig. 3 is that the nodes of the electric field for the harmonics of quarter wave are neither located at the equator nor are symmetric about the equator (they are either at the equator or symmetric about the equator in case of the half wave) but are biased towards the ionosphere with smaller Pedersen conductivity value. One can evaluate the Poynting flux to show the energy flow direction, as is rigorously discussed by Ozeke et al. (2005). However, the present model deals only with idealistic ionospheric boundary and thus cannot account for the Poynting flux.

The field line structure of magnetic field for these density variation are shown in Fig. 4. The top panels of Fig. 4 show the variation for density index $m = 4$, the middle panels show the variation for $m = 5$ and the bottom panels show the variation for density index $m = 6$. It clearly brings out the effect of plasma loading (i.e. m dependence) on magnetic field variation along a field line. There is definite departure between the magnetic field computed analytically from the numerical exact solution for the density variation of $m = 4$ (shown in top panel). However, with increasing m the departure in the field variations is seen to be reduced and for $m = 6$ the analytic structure is identical with that computed numerically.

For a given harmonic, the mode structures along the field lines depend on the ionospheric conductivities at the conjugate points. The condition $\Sigma_P^N \to 0$ leads to the formation of anti-node of electric field (Fig. 3) and node of magnetic field at the conjugate point in the northern hemisphere (Fig. 4).

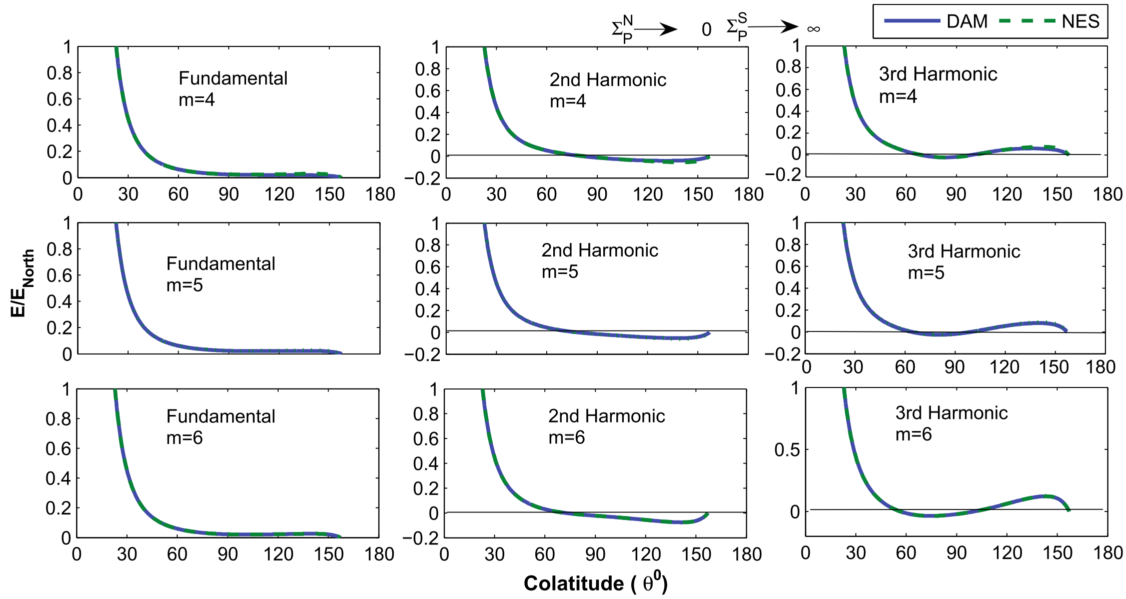

Fig. 3 Latitudinal structures of electric field for quarter wave toroidal oscillation for the first three harmonics obtained from DAM and numerical exact solution at $L = 6.6$. The ionopsheric conductivities were considered as $\Sigma_P^N \to 0$ and $\Sigma_P^S \to \infty$. The *top*, *middle* and *bottom panels* show the electric field variation along the field line for density indices $m = 4$, $m = 5$ and $m = 6$ respectively. The magnitude of electric field at any point can be obtained by multiplying with the indicated factor. E_{North} represents the value of electric field at northern conjugate point

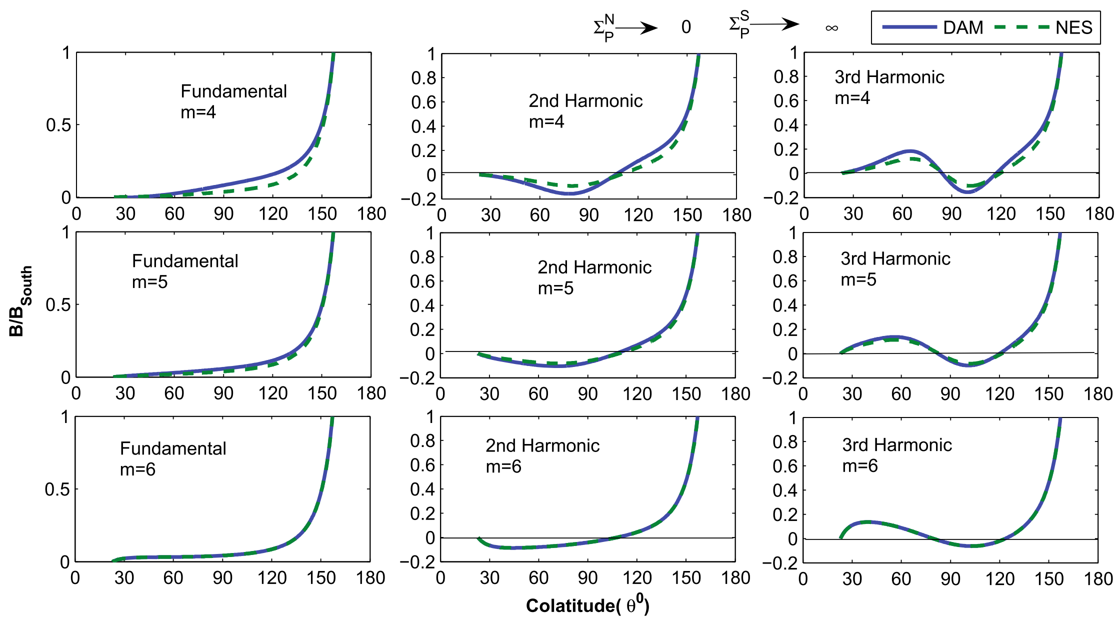

Fig. 4 Latitudinal structures of magnetic field for quarter wave toroidal oscillation for the first three harmonics obtained from DAM and numerical exact solution at $L = 6.6$. The ionopsheric conductivities were considered as $\Sigma_P^N \to 0$ and $\Sigma_P^S \to \infty$. The *top*, *middle* and *bottom panels* show the magnetic field variation along the field line for density indices $m = 4$, $m = 5$ and $m = 6$ respectively. The magnitude of magnetic field at any point can be obtained by multiplying with the indicated factor. B_{South} represents the value of magnetic field at southern conjugate point

This is reversed at the conjugate point in the southern hemisphere where $\Sigma_P^S \to \infty$ (refer Figs. 3 and 4). These results obtained from DAM and NES are consistent with earlier numerical results of Allan (1983).

4 Discussion and conclusions

While deriving Eq. (1) we have completely neglected the compression of the magnetic field fluctuation. If we take compression into account then the mode equation takes the form

$$\mu_o \rho \frac{\partial^2}{\partial t^2}\left(\frac{\xi_\alpha}{h_\alpha}\right) - \frac{1}{h_{\alpha^2}}\overrightarrow{B_o}.\overrightarrow{\nabla}\left[h_{\alpha^2}\overrightarrow{B_o}\cdot\overrightarrow{\nabla}\left(\frac{\xi_\alpha}{h_\alpha}\right)\right] = -\frac{B_0}{h_\alpha^2}\frac{\partial b_s}{\partial \alpha} \quad (7)$$

In Eq. (7), b_s is the magnetic field perturbation due to compression. The differentiation $\partial/\partial\alpha$ in the right hand side implies that the operation has to be performed with respect to longitude ϕ for the toroidal oscillation and with respect to ν for the poloidal oscillation. The directions of $\overrightarrow{\nabla}\phi$, $\overrightarrow{\nabla}\nu$ and $\overrightarrow{\nabla}s$ are respectively azimuthal, meridional and along the field line away from equator and ($\overrightarrow{\nabla}s$, $\overrightarrow{\nabla}\phi$, $\overrightarrow{\nabla}\nu$) form a right handed orthogonal system.

Any change in the magnetospheric current caused by an external forcing will result in a fluctuation b_s at the location of the field line. It can then act as a driver to cause a response in the normal modes of field line oscillations (Lee 1996). It should be noted that the normal modes (i.e. solution of Eq. (1)) act as a complimentary function in the complete solution of Eq. (7). Thus, it is of paramount importance to get the analytic structure of normal modes a priori. The present paper focuses on this aspect of toroidal quarter wave oscillations. The estimation of response of these modes to external driving fores will form the part of our future studies.

In both DAM and NES we have considered extreme ionospheric boundary conditions, i.e. the ionosphere at the one end is infinitely conducting and at the other end it is infinitely resistive. Since we have considered idealistic boundaries, the damping is neglected at the conjugate points.

From Fig. 4, it can be seen that the departure of analytically computed solution increases with decreasing density index. This is because as the density index decreases, the effect of singularity at ($\theta \sim 0$ and $\theta \sim \pi$) contained in the term $\phi(\nu)$ of Eq. (3) starts to affect the solution (Sinha and Rajaram 1997).

Despite these limitations in the present model, it is the only analytic model as of now that can address the temporal and spatial characteristics of quarter wave oscillations for generalized power variation of plasma density in the dipole field geometry. Hence, this model has a potential to be applied to different regions of the magnetosphere obeying different density distribution. A good agreement with the numerical exact solution in general and identical solution for $1/r^6$ type plasma distribution as given by earlier workers in particular, puts the model on firmer ground.

Quarter wave oscillations are mostly observed in solstices during dawn and dusk period when conjugate ionospheres are highly asymmetric. The observed frequency using satellite and ground data can be used in the model to compute the plasma density and thus the model can play an important part in plasma diagnostics in the Earth's magnetosphere. An all out attempt will be made to incorporate damping in the model in our future course of work.

Acknowledgements We thank Prof. R. Rajaram for thoughtful discussions on this work.

References

Allan, W., Knox, F.B.: A dipole field model for axisymmetric Alfvén wave with finite ionospheric conductivities. Planet. Space Sci. **27**, 79 (1979a)

Allan, W., Knox, F.B.: The effect of finite ionospheric conductivities on axisymmetric toroidal Alfvén wave resonances. Planet. Space Sci. **27**, 939 (1979b)

Allan, W.: Quarter-wave ULF pulsations. Planet. Space Sci. **31**, 323 (1983)

Anderson, B.J., Engebretson, M.J., Rounds, S.P., Zanetti, L.J., Potemra, T.A.: A statistical study of Pc3-5 pulsations observed by the AMPTE/CCE magnetic fields experiment 1. Occurrence distributions. J. Geophys. Res. **95**, 10,495 (1990)

Bender, C.M., Orszag, S.A.: Advanced Mathematical Methods for Scientists and Engineers. McGraw-Hill, New York (1978)

Bochev, A.Z., Sinha, A.K.: A coordinated study of field-aligned currents and Pc5 ULF waves during ejecta 1997. Adv. Space Res. **46**, 1111 (2010)

Budnik, F., Stellmacher, M., Glassmeier, K.H., Buchert, S.C.: Ionospheric conductance distribution and MHD wave structure: Observation and model. Ann. Geophys. **16**(2), 140 (1998)

Carpenter, D.L., Smith, R.L.: Whistler measurements of electron density in the magnetosphere. Rev. Geophys. **71**, 415 (1964)

Cummings, W.D., O'Sullivan, R.J., Coleman, P.J.: Standing Alfvén waves in the magnetosphere. J. Geophys. Res. **74**, 778 (1969)

Dungey, J.W.: Electrodynamics of the outer atmospheres. Rep. 69, Ions. Res. Lab. Pa. State Univ., University Park (1954)

Dungey, J.W.: In: Matsushita, S., Campbell, W. (eds.) Hydromagnetic Waves, in Physics of Geomagnetic Phenomena, p. 913. Academic Press, New York (1968)

Engebretson, M.J., Zanetti, L.J., Potemra, T.A., Acuña, M.H.: Harmonically structured ULF pulsations observed by AMPTE/CCE magnetic field experiment. Geophys. Res. Lett. **13**, 905 (1986)

Gallagher, D.L., Craven, P.D., Comfort, R.H.: Global core plasma model. J. Geophys. Res. **105**, 18,819 (2000)

Goldstein, J., Denton, R.E., Hudson, M.K., Miftakhova, E.G., Young, S.L., Menietti, J., Gallagher, D.: Latitudinal density dependence of magnetic field lines inferred from Polar plasma wave data. J. Geophys. Res. **106**, 6195 (2001)

Hughes, W.J., Southwood, D.J.: The screening of micropulsation signals by the atmosphere and ionosphere. J. Geophys. Res. **81**, 3234 (1976)

Klimushkin, D.Yu., Mager, P.N., Glassmeier, K.-H.: Toroidal and poloidal Alfvén waves with arbitrary azimuthal wave numbers in a finite pressure plasma in the Earth's magnetosphere. Ann. Geophys. **22**, 267 (2004)

Langer, R.E.: The asymptotic solutions of ordinary linear differential equations of second order, with special reference to a turning point. Trans. Am. Math. Soc. **67**, 461 (1949)

Lanzerotti, L.J., Southwood, D.J.: In: Lanzerotti, L.J., Kennel, C.F., Parker, E.N. (eds.) Hydromagnetic Waves, Solar System Plasma Physics, vol. III. North-Holland, Amsterdam (1979), p. Ill

Lee, D.-H.: Dynamics of MHD wave propagation in the low-latitude magnetosphere. J. Geophys. Res. **101**, 15,371 (1996)

Leonovich, A.S., Mazur, V.A.: A theory of transverse small-scale standing Alfvén waves in an axially symmetric magnetosphere. Planet. Space Sci. **41**, 697 (1993)

Leonovich, A.S.: A theory of field line resonance in a dipole-like axisymmetric magnetosphere. J. Geophys. Res. **106**, 25,803 (2001)

Liu, W., Cao, J.B., Li, X., Sarris, T.E., Zong, Q.-G., Hartinger, M., Takahashi, K., Zhang, H., Shi, Q.Q., Angelopoulos, V.: Poloidal ULF wave observed in the plasmasphere boundary layer. J. Geophys. Res. Space Phys. **118**, 4298 (2013). doi:10.1002/jgra.50427

Mager, P.N., Klimushkin, D.Yu.: On impulse excitation of the global poloidal modes in the magnetosphere. Ann. Geophys. **24**, 2429 (2006)

Mager, P.N., Klimushkin, D.Yu.: Generation of Alfvén waves by a plasma inhomogeneity moving in the Earth's magnetosphere. Plasma Phys. Rep. **33**, 391 (2007)

Mager, P.N., Klimushkin, D.Yu., Pilipenko, V.A., Schaefer, S.: Field-aligned structure of poloidal Alfvén waves in a finite pressure plasma. Ann. Geophys. **27**, 3875 (2009)

Mann, I.R., Wright, A.N.: Finite lifetimes of ideal poloidal Alfvén waves. J. Geophys. Res. **100**, 23,677 (1995)

Newbury, I.T., Comfort, R.H., Richard, P.G., Chappell, C.R.: Thermal He+ in the plasmasphere: Comparison of observations with numerical calculations. J. Geophys. Res. **94**, 15,265 (1989)

Obana, Y., Menk, F.W., Murray, D., Sciffer, Waters, C.L.: Quarter-wave modes of standing Alfvén waves detected by cross-phase analysis. J. Geophys. Res. **113** (A08203) (2008). doi:10.1029/2007JA012917

Orr, D.: Magnetic pulsations within the magnetosphere: A review. J. Atmos. Terr. Phys. **35**, 1 (1973)

Ozeke, L.G., Mann, I.R., Mathews, J.T.: The influence of asymmetric ionospheric Pedersen conductances on the field-aligned phase variation of guided toroidal and guided poloidal Alfvén waves. J. Geophys. Res. **110**, A08210 (2005). doi:10.1029/2005JA011167

Pilipenko, V.A., Mazur, N.G., Federov, E.N., Engebretson, M.J., Murr, D.L.: Alfvén wave reflection in a curvilinear magnetic field and formation of Alfvenic resonators on open field lines. J. Geophys. Res. **110**, A10S05 (2005). doi:10.1029/2004JA010755

Scholer, M.: On the motion of artificial ion clouds in the magnetosphere. Planet. Space Sci. **18**, 977 (1970)

Singer, H.J., Southwood, D.J., Walker, R.J., Kivelson, M.G.: Alfvén wave resonances in a realistic magnetospheric magnetic field geometry. J. Geophys. Res. **86**, 4589 (1981)

Sinha, A.K., Rajaram, R.: An analytic approach to toroidal eigen mode. J. Geophys. Res. **102**, 17,649 (1997)

Sinha, A.K., Rajaram, R.: Dominance of toroidal oscillations in dawn/dusk sectors: A consequence of solar wind pressure variation. Earth Planets Space **55**, 93 (2003)

Sinha, A.K., Yeoman, T.K., Wild, J.A., Wright, D.M., Cowley, S.W.H., Balogh, A.: Evidence of transverse magnetospheric field line oscillations as observed from Cluster and ground magnetometers. Ann. Geophys. **23**, 919 (2005)

Southwood, D.J., Kivelson, M.G.: Damping standing Alfvén waves in the magnetosphere. J. Geophys. Res. **106**, 10,829 (2001)

Takahashi, K., Hartinger, M.D., Angelopoulos, V., Glassmeier, K.-H., Singer, H.J.: Multispacecraft observations of fundamental poloidal waves without ground magnetic signatures. J. Geophys. Res. Space Phys. **118**, 4319 (2013). doi:10.1002/jgra.50405

Waters, C.L., Lysak, R.L., Sciffer, M.D.: On the coupling of fast and shear Alfvén wave modes by the ionospheric Hall conductance waves in the magnetosphere. Earth Planets Space **65**, 385 (2013)

Yagova, N., Pilipenko, V., Fedorov, E., Vellante, M., Yumoto, K.: Influence of ionospheric conductivity on midlatitude Pc3-4 pulsations. Earth Planets Space **51**, 129 (1999)